Impact of a large-scale replacement of maize by soybean on water deficit in Europe

Ronny Lauerwald, Nicolas Guilpart, Philippe Ciais, David Makowski

Impact of a Large-Scale Replacement of Maize by Soybean on Water Deficit in Europe

R. Lauerwald[1], N. Guilpart[2], P. Ciais[3] and D. Makowski[4]

[1]Université Paris-Saclay, INRAE, AgroParisTech, UMR Ecosys, 91120 Palaiseau, France.

[2]Université Paris-Saclay, AgroParisTech, INRAE, UMR Agronomie, 91120 Palaiseau, France.

[3]Laboratoire des Sciences du Climat et de l'Environnement, IPSL, CEA-CNRS-UVSQ, Université Paris-Saclay, 91190 Gif-sur-Yvette, France.

[4]Université Paris-Saclay, AgroParisTech, INRAE, UMR MIA PS, 91120 Palaiseau, France.

Corresponding author: Ronny Lauerwald (ronny.lauerwald@inrae.fr)

Abstract

The EU imports large quantities of soybeans, mainly for livestock feed. However, there is a trend to increase domestic soybean production and reduce imports. In this study, we investigate the potential impact of an increased EU soybean cultivation on evapotranspiration (ET), water deficit, and irrigation needs. We focus on the consequences of replacing maize with soybeans, as both crops have similar cropping periods and high water demands. We implement a simple, well established crop water model that estimates crop water deficit (*ETd*) as the difference between simulated potential (*ETc*) and actual (*ETa*) ET. We apply this model over the EU from 2001 to 2020, using data on daily reference ET and precipitation, soil hydrological properties and three different crop calendars. Results indicate that a maize-to-soybean conversion would result in an average *ETd* increase of 49.0±22.1 mm season^{-1} across the EU. In the four countries of France, Italy, Hungary and Romania, where most of the additional soybean production would be allocated, crop water deficits would increase on average by 21-34% compared to that of maize, following an increased *ETc* and/or decreased *ETa*. However, the decrease in *ETa* is largely due to an assumed shorter root depth for soybean, while recent empirical results suggest that both crops may actually have comparable root depths. Using the same root depth for maize and soybean, the simulated average increase in *ETd* amounts to only 28.2±18.3 mm season^{-1}. Our results are sensitive to the choice of crop calendar, with reduced *ETd* for later sowing dates .

Keywords

soybean; maize; crop water deficit; Europe; evapotranspiration; modeling

1 Introduction

The European Union is importing about 30 Mt of soybean per year from the US and South America, mainly for livestock feed (Debaeke et al., 2022). There is however a growing awareness that these soybean imports drive agricultural conversion of savannahs and forests in South America (Fearnside, 2001; Nepstad et al., 2014). Soybean production in the US, on the other hand, is dominated by genetically modified (GM) cultivars (Harlander, 2002). On the consumer side, there is a growing demand for soybean produced under environmentally friendly conditions, which could be fulfilled by an increased domestic production of soybeans in the EU (Zander et al., 2016). Indeed, although only 3% of soybean consumption in the EU is currently covered by domestic production (Zander et al., 2016), soybean production has experienced a significant growth in the EU over the last two decades. While in the years 2007-2009 the production in EU27 was below 1 Mt soybean yr^{-1}, it reached 2.4-2.9 Mt soybean yr^{-1} in the years 2015-2021 (European Commission, 2022). Over the same period, the soybean cultivated area increased from 0.3-0.4 million ha to 0.8-1.0 million ha, respectively (European Commission, 2022). The EU supports the expansion of soybean and other leguminous crops in the framework of the Farm2Fork strategy, which forms the central element of the European Green Deal to achieve climate neutrality of EU agriculture by 2050, and which takes into account impacts on the climate system caused outside of EU borders (European Commission, 2020).

In a recent study, Guilpart et al. (2022) have demonstrated the possibility to increase European domestic soybean production substantially, satisfying at least half of the current demand in Europe. Such an expansion of soybean cultivation may have environmental and agronomic benefits. As a nitrogen-fixing crop, the integration of soybean into crop rotations may reduce the amount of nitrogen fertilizers applied and increase the yield of the following crop (Zander et al., 2016; Cernay et al. 2018). On the other hand, potential disadvantages of soybean cultivation are

related to high water demands (Grassini et al., 2015, Rüdelsheim and Smets, 2012) that may increase agricultural water consumption for irrigation, or reduce groundwater recharge over agricultural land. This impact of a soybean area expansion on the water cycle still needs to be assessed at European scale to get a more complete picture on the potential advantages and disadvantages of decreasing European soybean deficiency. On average, agriculture is responsible for about one fourth of the water consumption in the EU, but becomes the dominant consumer in southern countries of the EU and during summer months where/when crops have highest irrigation needs, but also when the availability of surface water for abstraction is lowest (Kristensen et al., 2018). EU environmental policies aim at preserving quantity and quality of renewable freshwater resources (Kristensen et al., 2018), for which an intensification of irrigation activities should be avoided as far as possible. On the other hand, the agronomic benefits to irrigate soybean in Europe has been demonstrated as well, with yield increases of ~40% under supplementary irrigation in Germany (Karges et al., 2022). Thus, it is possible that decreasing soybean deficiency in Europe may go hand in hand with intensified irrigation.

In this study, we analyzed the potential impact of soybean expansion in Europe on crop water deficit, irrigation demands and renewable freshwater resources. Following Martin (2015), we assume that cultivation of soybeans expands primarily at the expense of maize, which is a similarly thermophile and water demanding summer crop, and which is also mainly cultivated as animal feed in the EU, although taking a different role in the diet of livestock (Karlsson et al. 2021). Note further that about 20% of the maize cultivated in the EU is already irrigated (Zajac et al., 2022). Moreover, we assume that soybean will often be planted in rotations with maize, which was shown to be a favorable combination with agronomical and ecological benefits (Behnke et al., 2018; Grassini et al., 2015). Our assumption that the expansion of soybean cultivation will mainly occur at the expense of maize is finally supported by similar developments in the US during the mid-20th century (Langthaler, 2020). We simulate crop water requirements of soybean vs. maize across Europe over the last two decades, using the model-based approach developed by Allen et al. (1998) for the FAO (FAO56) and agricultural climate and soil datasets developed by the Joint Research Centre of the EU. The FAO56 approach has proven to be relevant for estimating potential and actual evapotranspiration (ET) of a wide variety of crops. Due to its simplicity and efficiency, this approach has been implemented in many software packages to support the planning of irrigation at field scale, as summarized in the review by Pereira et al. (2020). The study by Sieber & Döll (2010) has demonstrated that this approach can as well be applied at global scale.

We simulate the difference in crop water deficits for maize vs. soybean in Europe, for the areas where a replacement of maize by soybean would be most productive according to the projections of expected soybean yields by Guilpart et al. (2022). Finally, we critically evaluate the modeling approach using three alternative crop calendars and performing a sensitivity analysis with changing parametrisation of root depth, sowing and harvest date, and coefficients controlling the theoretical crop water needs.

2 Materials and Methods

2.1 Model Description

Our model estimates daily potential and actual evapotranspiration (ET) based on the well-established FAO56 double crop coefficient method (Allen et al., 1998). It requires daily values of precipitation and reference ET (ET0) as inputs. ET0 is defined as potential ET of a hypothetical reference crop similar to a well-watered, actively growing grassland with an

uniform height of 12 cm. ET0 is directly available from agrometeorological datasets such as the one used in this study (see section 2.2). It was calculated using standard approaches such as the Penman-Monteith equation (Allen et al., 1998). Our model operates in two major steps: First, it calculates crop specific potential ET (*ETc*) from ET0 based on prescribed, ideal crop phenology (section 2.1.1). Second, it calculates the actual ET (*ETa*) from *ETc* based on a simple crop soil water budget model accounting for changing soil water storage through inputs of precipitation (*P*), and losses through ET, surface runoff and deep percolation (section 2.1.2).

2.1.1 Simulation of Crop-Specific Potential ET (*ETc*)

Allen et al. (1998) proposed two different strategies to derive *ETc* from ET0 based on either a single or a double crop coefficient. The first strategy uses a single crop coefficient *Kc* (eq. 1) to compute *ETc* from ET0. Standard values of *Kc* were derived from empirical studies as shown by Allen et al. 1998 (see below Table 1). In this approach, the growing season is divided into four consecutive crop growth stages: 1) initial stage from sowing until about 10% of vegetation cover (defined as fraction of ground covered by photosynthetically active vegetation) is reached; 2) the stage of crop development from ~10% vegetation cover to effective full cover; 3) the mid-season stage until the beginning of senescence; and 4) late season stage until harvest. Stage 3 covers the phenological stages of flowering, fruit development, and ripening of fruit and seeds (growth stages 6-8 on the BBCH scale), while stage 4 represents the phenological stage of senescence (stage 9 on the BBCH scale). For a given crop, *Kc* evolves over the growing period as follows. During stage 1, *Kc* remains at the initial value. During stage 2, *Kc* increases linearly from the initial to the mid-season value. During stage 3, *Kc* remains at the mid-season value. Finally, during stage 4, it linearly decreases to the end of the season value.

For our model, we used a second strategy based on the double crop coefficient approach proposed by Allen et al. (1998), which allows us to estimate evaporation and transpiration separately, as required to simulate the actual, water limited ET (see section 2.1.2). The crop coefficient *Kc* is split into the coefficients *Ke* and *Kcb* (eq. 2, Figure 1) to estimate potential evaporation *Ec* (eq. 3) and potential transpiration *Tc* (eq. 4) from ET0, respectively. Note that in our model set-up, *Ke* assumes no water limitation, and is thus the coefficient leading to *Ec*. As for *Kc*, tabulated values for *Kcb* were simply adopted from Allen et al. (1998), and *Ke* was calculated as the difference between these coefficients (see Table 1). Outside of the growing season, for which we assume bare soil, *Kcb* is zero and *Ke* is set to base-value of 0.30, following Allen et al. (1998).

$$ETc = Kc * ET0 \quad \text{(eq. 1)}$$

$$Kc = Kcb + Ke \quad \text{(eq. 2)}$$

$$Ec = Ke * ET0 \quad \text{(eq. 3)}$$

$$Tc = Kcb * ET0 \quad \text{(eq. 4)}$$

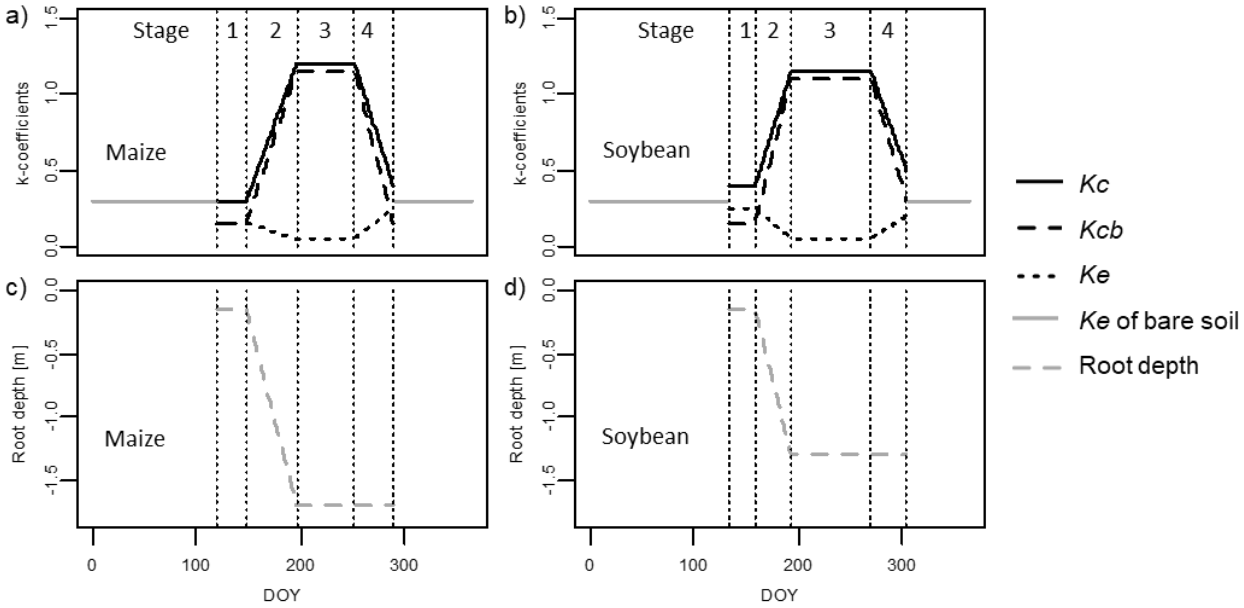

Figure 1. Example of Crop Coefficients and Root Depth for Maize (a, c) and Soybean (b, d) over the Annual Cycle and the Four Growing Stages from Sowing to Harvest**.** DOY: day of year.

Table 1. Crop Coefficients after Allen et al. (1998).

Stage	Maize			Soybean		
	Kc	*Kcb*	*Ke*	*Kc*	*Kcb*	*Ke*
1	0.30	0.15	0.15	0.40	0.15	0.25
3	1.20	1.15	0.05	1.15	1.10	0.05
end of 4	0.40	0.15	0.25	0.50	0.30	0.20

Table 2. Relative Length of Growing Stages (after Sieber and Döll 2010) Expressed in Proportion of the Length of the Growing Season.

	stage 1	stage 2	stage 3	stage 4
Maize	0.17	0.28	0.33	0.22
Soy	0.15	0.20	0.45	0.20

The length of the different crop growth stages varies not only among crop types, but also depending on cultivar, climate and sowing date (Allen et al. 1998). Here, we adopted the approach implemented by Siebert and Döll (2010) for their application at the global scale where the length of each crop stage changes proportionally to the total length of the growing season defined according to different crop calendars (see section 2.2).

2.1.2 Simulation of Actual Evapotranspiration

The soil water budget model is based on a representation of the soil column as two interconnected compartments, a topsoil compartment and a subsoil compartment with corresponding soil water storages S_{top} and S_{sub}, respectively. For both compartments, the daily change in soil water storage is simulated. S_{top} and S_{sub} are represented in units of mm. The depth of the soil column D_{soil} equals the maximum root depth, which is set at 1.7 m for maize and at 1.3

m for soy following Allen et al. (1998). For the depth of the topsoil, we adopted the value of D_{top} = 0.15 m suggested by Allen et al. (1998). The depth of the subsoil D_{sub} is then simply derived as difference between D_{soil} and D_{top}.

Under the rain-fed conditions considered in our study, the topsoil compartment receives water inputs from infiltrating precipitation (eq. 5) equal to the difference between total daily precipitation *P* and surface runoff *R*. The top-soil loses water from actual evaporation *Ea* (Ea_{top}) and actual transpiration *Ta* (Ta_{top}), but also from percolation to the sub-soil compartment (*DI*). The sub-soil compartment receives infiltrating water from the top soil (*DI*) as only input (eq. 6). Water loss from the subsoil is due to transpiration (Ta_{sub}) and deep-percolation (*DP*) of water out of the root-zone. Note that *Ea* only occurs from the topsoil. For all fluxes of water, we use units of mm d^{-1}.

$$\Delta S_{top} = (P\text{-}R) - Ea_{top} - Ta_{top} - DI \quad \text{(eq. 5)}$$

$$\Delta S_{sub} = DI - Ta_{sub} - DP \quad \text{(eq. 6)}$$

Surface runoff *R* is calculated based on the curve number approach described in the USDA National Engineering Handbook (USDA NRCS, 2004). This simple and robust approach has been used for decades, and was implemented into many contemporary crop water models like BUDGET (Raes et al., 2006), BEACH (Sheikh et al., 2009), SIMDualKc (Rosa et al., 2016), and AquaCrop (Raes et al., 2009). Deep infiltration *DI* occurs when the water storage of the top soil exceeds field capacity *FC* (given as volumetric water content), and is simply calculated as the difference between actual topsoil water content and topsoil water content at *FC* (eq. 7). The topsoil water content at *FC* is calculated by multiplying *FC* by the depth of the topsoil D_{top}. Similarly, deep percolation *DP* occurs when the water storage in the subsoil exceeds *FC*, and then equals the amount of water storage in excess (eq. 8). The subsoil water content at *FC* is calculated by multiplying *FC* by the depth of the subsoil column D_{sub}.

$$DI = S_{top} - FC \cdot D_{top} \quad \text{(eq. 7)}$$

$$DP = S_{sub} - FC \cdot D_{sub} \quad \text{(eq. 8)}$$

To calculate the actual evaporation *Ea* and transpiration *Ta*, we also follow Allen et al. (1998). *Ea* is limited by the actual water storage in the topsoil, and this effect is expressed by the unitless reduction factor *Kr* (eq. 9, 10). The minimum top soil water storage that can be reached until no evaporation occurs anymore is defined as half of the topsoil water storage at the permanent wilting point *PWP* (Allen et al., 1998). Note that other traditional large-scale approaches to model soil hydrology simply assume that soil moisture cannot drop below *PWP* (e.g. MacBean et al. 2020). However, empirical evidence exists that soil evaporation can drive topsoil moisture well below *PWP* in dryer climates (Agam et al., 2004), and assuming half of *PWP* as minimum limit for *Ea* appears thus more reasonable. *Kr* is calculated as the ratio between the actual amount of water that is available for evaporation and the maximum possible amount of water that could be available for evaporation (eq. 10), the latter being defined as difference between topsoil water storage at *FC* and half the topsoil water storage at *PWP*. Further, the amount of water in the topsoil, which is readily available for evaporation (readily evaporable water – *REW*), is taken into account in this equation. Note that *REW* refers to total amounts of water expressed

in mm, and does not represent volumetric water contents as *FC* and *PWP*. Values of *FC* and *PWP* are computed from spatial input data (section 2.2). Values of *REW* are estimated from the values of *FC* and *PWP*, which is possible as all three parameters depend mainly on soil texture.Allen et al. (1998) gives tabulated values for *REW*, *FC*, and *PWP* for different soil texture classes. Based on these tabulated data, we fitted eq. 11 which relates *REW* in mm to *FC* and *PWP* as volumetric water content (RMSE=0.6mm, rRMSE=7%). The empirical coefficient 0.60 in this equation was accurately estimated (standard error of 0.01). We thus assume that the so estimated *REW* values are reasonable and consistent with the *FC* and *PWP* values used as model input.

$$Ea = \min(Kr*Ec\ , S_{top} - 0.5*PWP*D_{top}) \qquad \text{(eq. 9)}$$

$$K_r = min\left(\frac{S_{top} - 0.5 \cdot PWP \cdot D_{top}}{(FC - 0.5 \cdot PWP) \cdot D_{top} - REW}, 1\right) \qquad \text{(eq. 10)}$$

$$REW = 0.60 \cdot (FC - PWP) \qquad \text{(eq. 11)}$$

Ta reduces water content in both the top- and subsoil, depending on root depth D_{root} that changes over the season of crop growth. For stage 1, we assume that the roots are entirely within the topsoil, and no water is taken from the sub-soil (D_{root}=D_{top}). During stage 2, root depth linearly increases from D_{top} to D_{soil}, which equals the crop specific maximum root depth (see Figure 1c,d). During stage 3 and 4, D_{root} equals D_{soil}. Outside of the growing season, *Ta* is zero.
Similarly to *Ea*, *Ta* is scaled to *Tc* based on a reduction factor, *Ks*, which depends on the ratio of actual water storage in the root zone S_{root} which is in excess to *PWP*, and the available water capacity, i.e. the difference between *FC* and *PWP*, over D_{root} (eqs. 12,13). The maximum possible value of *Ta* (eq. 12) is defined as the difference between the actual amount of water stored in the root zone S_{root} and the water storage over D_{root} at *PWP*, from which further the amount of water already lost to *Ea* is subtracted. S_{root} includes at least S_{top}, and the part of S_{sub} that is penetrated by roots (eq. 14). The calculation of *Ks* depends further on the daily values of *ETc (ETc=Tc+Ec)* (eq. 15) and a crop specific parameter *pstd*, which equals 0.55 and 0.50 for maize and soybean, respectively (Allen et al. 1998). The amount of transpired water that is taken from the top- (Ta_{top}) vs. subsoil (Ta_{sub}) (eqs. 5, 6) is linearly scaled to the proportion of S_{root} that can be attributed to the corresponding part of the soil column. Finally, *ETa* is calculated as the sum of *Ta* and *Ea* (eq. 16), and the crop water deficit *ETd* is calculated as the difference between *ETc* and *ETa* (eq. 17).

$$T_a = min(Ks \cdot Tc, S_{root} - PWP \cdot D_{root} - E_a) \qquad \text{(eq. 12)}$$

$$K_s = min\left(\frac{S_{root} - PWP \cdot D_{root}}{(1-p) \cdot (FC - PWP) \cdot D_{root}}, 1\right) \qquad \text{(eq. 13)}$$

$$S_{root} = S_{top} + S_{sub} \cdot \frac{D_{root} - D_{top}}{D_{soil} - D_{top}} \qquad \text{(eq. 14)}$$

$$p = pstd + 0.04 \cdot \left(5.0 - (Tc + Ec)\right) \qquad \text{(eq. 15)}$$

$$ETa = Ta + Ea \quad \text{(eq. 16)}$$

$$ETd = ETc - ETa \quad \text{(eq. 17)}$$

2.2 Model Input Data at European Scale

The model is applied at European scale using daily agroclimatology forcing data from JRC (see Table 3 for reference, see Figure S1 giving overall workflow). More precisely, we use the daily values of precipitation and ET0 over the period 1999-2020 available in this database. We adopted the grid defined by the spatial reference and resolution (25km) of this dataset for our simulations.

Information on permanent wilting point (*PWP*) and field capacity (*FC*) of soils was taken from the high resolution (1 km) 3D soil hydraulic database provided by Tóth et al (2017) (see Table 3). The values of these parameters were first averaged over the soil profile for each 1 km grid cell. To extract values representative for agricultural soils, this high resolution grid was then masked by the areas of managed lands extracted from the GlobCOVER v2.3 dataset (Arino et al., 2012), which is representative for the year 2009, before we calculated the arithmetic means of *PWP* and *FC* for each 25 km cell of our model grid.

Each model grid cell was assigned to one of four soil hydraulic classes (< 10%, 10-20%, 20-40%, >40% of clay, USDA NRCS 2004) which were required for the curve number approach we used to estimate runoff in response to precipitation and soil moisture. For this, we first calculated the average soil clay content per 25 km cell using the highly resolved information from the Harmonized World Soil Database (HWSD) (Nachtergaele et al., 2010). Then, we classified the grid cells accordingly.

Finally, we extracted data on sowing and harvest dates of soybean and maize from three different crop calendars: MIRCA (Portmann et al., 2010), JRC-crop calendar (Sacks et al., 2010), and the crop calendar of phase 3 the global gridded crop model inter-comparison project GGCMI (Jägermeyr et al., 2021), and assigned those information to each of the 25 km modelling grid cells (Figures S1-S3). For the preparation of the spatial data sets, we used ESRI™'s ArcGIS 10 with the SpatialAnalyst™ extension.

Table 3. Data Sets Used in this Study.

Parameters	Data source	Resolution
Daily ET0, *P*	JRC MARS Meteorological Database v.3.1, https://agri4cast.jrc.ec.europa.eu/dataportal/	25 km
PWP, *FC*	3D soil hydraulic database (Tóth et al., 2017), https://esdac.jrc.ec.europa.eu/content/3d-soil-hydraulic-database-europe-1-km-and-250-m-resolution	1 km
Cropland mask	GlobCOVER v2.3 dataset (Arino et al., 2012), http://due.esrin.esa.int/page_globcover.php	0.3 km
Clay content	Harmonized World Soil Database (Nachtergaele et al. 2010), https://pure.iiasa.ac.at/id/eprint/17595/	~1 km
Crop calendars	MIRCA (Portmann et al., 2010), https://www.uni-frankfurt.de/45218023/MIRCA	~10 km
	JRC (Sacks et al., 2010), https://sage.nelson.wisc.edu/data-and-models/datasets/crop-calendar-dataset/	~10 km
	GGCMI (Jägermeyr et al., 2021), https://zenodo.org/record/5062513#.Yv-T-d869aQ	~55 km

Actual expected soybean yields	Guilpart et al. (2022), https://zenodo.org/record/6136216#.Yv-UMt869aQ	~10 km
Annual maize area	JRC (2017) Yearly modeled crop area in EU v1.0, https://agri4cast.jrc.ec.europa.eu/dataportal/	25 km

2.3 Simulation Protocol

We ran simulations for each of the three crop calendars. While the most recent one (GGCMI) gives a single calendar date for sowing and harvest per grid cell and per crop species, MIRCA provides months of sowing and harvest time without further specifying the day of the month, and the JRC crop calendar gives explicit ranges of possible sowing and harvest dates, as well as the usual length of the growing season. For MIRCA and JRC crop calendar, we ran simulations for three different scenarios: 1) starting at the earliest possible day of sowing, 2) starting at the latest possible day of sowing, and 3) starting in the middle of the sowing period. For each crop calendar and grid cell, we assumed the same length in days of the growing period across all scenarios. For the JRC crop calendar, the lengths were explicitly given, but for the MIRCA dataset, the length of the growing periods was assumed equal to the length from the middle of the month of sowing to the middle of the month of harvest. Accordingly, we ran simulations using up to three different lengths of growing season (i.e. one for each of the three crop calendars) and up to seven different sowing dates (see Table 5 and Figures S2-S4).

Simulations were run over the period 1999 to 2020. As initial conditions at the beginning of the simulation, soil moisture in both top and subsoil was assumed to be at field capacity. The changes in these storages were then simulated over the full 22-year period depending on inflows and outflows at daily time-step. Daily outputs of *Tc*, *Ec*, *Ta*, *Ea*, *R*, and *DP* were aggregated to totals per year and season. To avoid any possible impact from the starting conditions chosen for the simulation, the first two years of simulation were discarded from the analysis, retaining only simulation results for the 20-year period 2001-2020.

2.4 Analysis of model simulations

2.4.1 Identification of potential areas for a maize-to-soybean conversion

To identify the areas where a maize-to-soybean conversion would be efficient to increase soybean production, we combined two datasets (Table 3): (i) the European map of simulated actual soybean yields under historical (1981-2010) rainfed conditions established by Guilpart et al. (2022) (Figure 2a), and (ii) the European map of maize cultivated areas for the years 1975-2017 (JRC 2017) (Figure 2b). To ensure spatial consistency, we calculated for each grid cell of our modelling grid the average predicted soybean yield from the finer grid cells of the map by Guilpart et al. (2022). In contrast, the European map of maize cultivated areas was used directly because it was based on the same spatial grid as the one used for our simulations.

We assumed a maize-to-soybean conversion likely to occur where maize is currently grown and simulated soybean yield is equal or higher than 1.5 t $ha^{-1}yr^{-1}$. This choice is consistent with the study of Guilpart et al. (2022) that chose this minimum threshold to identify suitable areas for soybean cultivation. Model outputs were then analyzed for the four countries that contain 80% of areas meeting these criteria: France, Italy, Hungary, and Romania (Figure 2). To explore the full potential of a maize-to-soybean conversion, we considered for each model grid cell the maximum maize area across the time period 2000-2017.

2.4.2 Effect of maize-to-soybean conversion on crop water deficit

The effects of maize-to-soybean conversion on crop water deficit were analyzed through three key parameters: *ETc*, *ETa*, and *ETd* during the growing season. We computed these three parameters for both soybean and maize, and then changes in these parameters if maize is converted to soybean ($\Delta ETc_{m\rightarrow s}$, $\Delta ETa_{m\rightarrow s}$, and $\Delta ETd_{m\rightarrow s}$, see eq. 18 as example for $\Delta ETd_{m\rightarrow s}$). First, we analysed these parameters calculating averages (over gridcells) per country, year and crop calendar scenario, weighted by the maize areas to be converted to soybean. Then, we calculated ensemble means, i.e. averages per year and country, to analyse the interannual variability (IAV), which we expressed as standard deviation σ_{IAV}. In addition, we calculate standard deviations between the multi-annual averages of all parameters per country and crop calendar scenario (σ_{CC}) as a measure of uncertainty related to this model input. We used a paired t-test to check whether differences in *ETd* under soybean vs. maize were significant.

We analyzed the impact of crop calendar choice in more detail over the model grid, quantifying the effects of changes in sowing date (Δt_{plant}) and season length (Δt_{seas}) on simulated $\Delta ETd_{m\rightarrow s}$, $\Delta ETc_{m\rightarrow s}$, and $\Delta ETc_{m\rightarrow s}$. First, we calculated the average $\Delta ETd_{m\rightarrow s}$, $\Delta ETc_{m\rightarrow s}$, and $\Delta ETc_{m\rightarrow s}$ over the period 2001-2020 for each grid cell and for any possible combination of the seven crop calendar scenarios specified above (section 2.3). This yielded each 113,778 pairs of either $\Delta ETd_{m\rightarrow s}$, $\Delta ETc_{m\rightarrow s}$, and $\Delta ETc_{m\rightarrow s}$ as dependent variable and Δt_{plant} and Δt_{seas} as predictors. Then, we use multiple linear regression with random effect to quantify the effects of Δt_{plant} and Δt_{seas} on the independent variables and to calculate the corresponding partial correlations.

2.5 Sensitivity analysis of model simulations to parameters

Finally, we performed a deeper evaluation of our model approach, testing how sensitive simulation results were to different model parameters. There are three different groups of model parameters that determine the differences in *ETa*, *ETc*, and *ETd* between soybean and maize: (i) crop coefficients (*Kc*) (Tables 1 and 2), (ii) root depths (D_{root}), and (iii) crop calendars (*CC*). $\Delta ETa_{m\rightarrow s}$, $\Delta ETc_{m\rightarrow s}$, $\Delta ETd_{m\rightarrow s}$ can be broken down into the effects of each of these three groups of model parameters. For instance, $\Delta ETd_{m\rightarrow s}$ can be broken down into $\Delta ETd_{m\rightarrow s,Kc}$, $\Delta ETd_{m\rightarrow s,Droot}$, and $\Delta ETd_{m\rightarrow s,CC}$. To calculate these effects, we ran for each of these three groups of model paratemers an alternative simulation for soybean with the corresponding model parameters set to the values used for maize. Then, we calculated the effects of each group of model parameters as differences between results from the standard simulation for soybean and the results from the corresponding alternative simulation for soybean, as demonstrated for the example of $\Delta ETd_{m\rightarrow s,Droot}$ in eq. 19, where $ETd_{s+Droot,m}$ represents the simulated *ETd* for soybean using the root depth of maize. We performed these alternative simulations and sensitivity analyses using the crop calendar GGCMI.

$$\Delta ETd_{m\rightarrow s} = ETd_s - ETd_m \quad \text{(eq. 18)}$$

$$\Delta ETd_{m\rightarrow s,Droot} = ETd_s - ETd_{s+Droot,m} \quad \text{(eq. 19)}$$

3 Results

3.1 Simulated Crop Water Needs, Consumption and Deficit

3.1.1 Multi-year averages

Guilpart et al. (2022) predicted that soybean yields could reach 3.3 t ha^{-1} yr^{-1} in some regions of Europe (Figure 2a), which is consistent with actual yield observations in Europe (European

Commission, 2022) considering growing regions with less than 1% irrigated area (MIRCA crop calendar). Considering only areas where a potential average soybean yield ≥1.5 t $ha^{-1}yr^{-1}$ was predicted and where maize was grown between 2000 and 2017 (Figure 2b), we estimated a potential increase in soybean production in the EU by 21.5 Mt yr^{-1}, i.e. ~70% soybean consumption in the EU. This would be more than seven times higher than the maximum total soybean production of 2.9 Mt yr^{-1} reported so far within the EU for the year 2018 (European Commission, 2022). About 80 % of this additional soybean production replacing maize could be attributed to France (4.5 Mt yr^{-1}), Italy (3.4 Mt yr^{-1}), Romania (6.2 Mt yr^{-1}) and Hungary (3.1 Mt yr^{-1}).

Panels c and d in Figure 2 show average seasonal crop water deficit for soybean (ETd_s) and maize (ETd_m), respectively. The spatial patterns in average *ETd* are very similar for both crops, with a tendency for southward increasing values and highest *ETd* in Spain and Southern Italy. Simulation results show that a maize-to-soybean conversion would increase *ETd* in 97.8 % of current maize area, with exceptions mainly found in Spain and Portugal (Figure 2e). The statistics of *ETa*, *ETc* and *ETd* under both crops in France, Italy, Hungary and Romania are listed in Table 4. We find higher average *ETd* under soybean than under maize in all four countries, with a national average predicted increase $\Delta ETd_{m\rightarrow s}$ ranging from +44 mm $season^{-1}$ in Italy to +64 mm $season^{-1}$ in Romania (Table 4). The paired t-test proves that for each of the four countries the differences between ETd_s and ETd_m is highly significant ($p<0.001$), with a 95% confidence interval around those mean values of less than ±6 mm $season^{-1}$ (Table S4). Moreover, taking for each of the four countries the 140 combinations of years (n=20) and crop calendar scenarios (n=7) as a reference, $\Delta ETd_{m\rightarrow s}$ is positive in 91% of the cases for Italy, in 98% of the cases in France and Hungary, and in all cases in Romania. In Hungary and Romania, increased *ETd* under soybean (+55 and +64 mm $season^{-1}$, respectively) appears to be mainly driven by increased *ETc* ($\Delta ETc_{m\rightarrow s}$ of +49 and +64 mm $season^{-1}$, respectively) (Table 4). On the contrary, in Italy and France, lower *ETa* values ($\Delta ETa_{m\rightarrow s}$ of -40 and -38 mm $season^{-1}$, respectively) appear to be the main reason for higher *ETd* under soybean ($\Delta ETd_{m\rightarrow s}$ of +44 and +50 mm $season^{-1}$, respectively), while in Hungary or Romania the differences between mean *ETa* of both crops are small or not significant, respectively (Table S4). Note that compared to France and Italy, the average annual precipitation *P* is roughly about 200 mm yr^{-1} lower in Hungary and Romania (Table 4), which may explain why *ETa* values are similar for both crops.

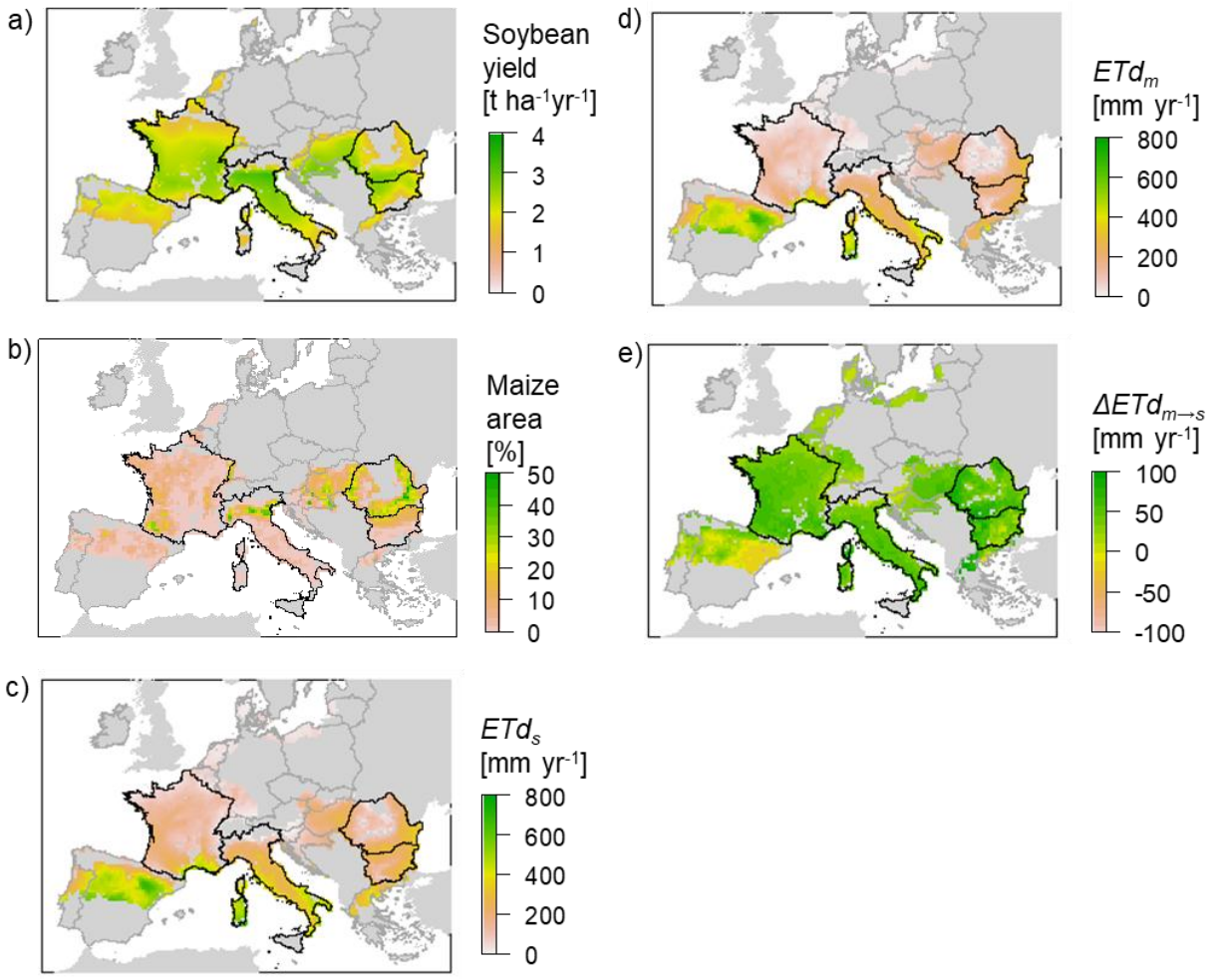

Figure 2. Maps of (a) Predicted Soybean Yield (Guilpart et al., 2022) under Historical Climate (1981-2010), (b) Maximum Areal Proportion of Maize Crop across EU (2000-2017), and Simulated Crop Water Deficit (2001-2020) under (c) Soybean (ETd_s) and (d) Maize (ETd_m), and (e) the Predicted Change in Crop Water Deficit when Maize is Converted to Soybean ($\Delta ETd_{m\rightarrow s}$).*

*All maps are masked to areas where maize was grown during 2000-2017, and where predicted soybean yield ≥1.5 t $ha^{-1}yr^{-1}$. The simulated crop water deficits represent the ensemble mean of the 7 different crop calendar scenarios. Dark grey lines give borders of EU27 countries (excl. Cyprus). Black lines give the boundaries of France, Italy, Hungary and Romania (from left to right), where most of the crop substitution is anticipated.

3.1.2 Inter-annual variability and seasonality

Figure 3 shows the time series of simulated *ETd*, *ETc* and *ETa* for soybean and maize in France, Italy, Hungary and Romania over the period 2001-2020, with means and min-max values obtained from the seven different crop calendar scenarios. Table 4 lists the ensemble means, the interannual variability of simulations (IAV) measured by σ_{IAV} as well as the uncertainty related to crop calendar choice measured by σ_{CC} for these four countries. We see that the IAV in *ETd* follows that of *ETc* (Figure 3), but is higher than that of *ETc* (Table 4). This is because *ETd* is

calculated as the difference between in-season *ETc* and *ETa*, while year-to-year variations in these two variables show strong negative correlations (Table 4). These negative correlations reflect the fact that *ETc* is higher in warm and dry years characterized by low soil moisture and insufficient precipitation to sustain an elevated *ETa*.

For Italy, Hungary and Romania, we find significant correlations between the annual values of *ETa*, *ETc*, and *ETd* vs. annual precipitation *P* (Table 4). For France, these correlations are not significant ($p>0.05$) for soybean. This may be related to the fact that France shows the lowest IAV for *P*, *ETa* and *ETd* among these four countries. For all four countries and both crops, we find that the IAV in *P* is much more important than IAV in *ETa*, *ETc* and *ETd*, and that its correlations with ETa, ETc, and ETd are often significant, but substantially lower than one (Figure 3). Nevertheless, σ_{IAV} of *ETd* is important, and amounts to about one third of the mean *ETd* for soybean, and ranges between one third (Italy) and one half (Hungary) of the mean *ETd* for maize (Table 4). But also the σ_{IAV} of $\Delta ETd_{m\rightarrow s}$, is important and ranges from one fifth (Romania) to one half (Italy) of the average $\Delta ETd_{m\rightarrow s}$. Interestingly, for none of the four countries does IAV in $\Delta ETd_{m\rightarrow s}$ show any significant correlations with *ETd* of any of the two crops.

To better understand the effect of differences in *P* on *ETa* and *ETd*, we have looked at both interannual and seasonal variations in fluxes (Figure 4). For detailed statistics of seasonal and interannual variability, see Table S1 in the supplemental information. A large fraction of annual *P* falls during the fallow period (Figure 4a,e). Moreover, the higher average annual *P* in France and Italy compared to Hungary and Romania is largely due to *P* during the fallow period, while during the four stages of crop growth considered in our model, the differences in average *P* per country are small compared to the IAV. More importantly, seasonality and interannual variability of losses of water to surface runoff *R* and deep percolation *DP* are strongly driven by *P*. If we subtract *R* and *DP* from *P* to get the net input of water that is available for *ETa* (P^*, Figure 4b,f), we find that contribution of the fallow period to this net input is substantially reduced compared to *P*. Moreover, the IAV and the differences in average P^* among the four countries are strongly reduced compared to *P*.

The contribution of the fallow period to annual *ETa* is small (Figure 4c,g). During this period, P^* generally exceeds *ETa*, which means a gain in soil moisture. In contrast to the large differences in average *P* during that period among the four countries, the average gain of soil moisture during the fallow period ranges between 104 mm in Romania to 130 mm in France for soybean. For maize, average fallow period soil moisture gain is higher and ranges from 128 mm in Romania to 182 mm in France. In contrast, *ETa* exceeds P^* over the four stages of crop development for both crops, which means that the soil moisture content is diminished during the growing period. During the third (flowering, fruit development, and ripening of fruit and seeds) and fourth stage (senescence to harvest), *DP* is zero (Table S1), which indicates that soil moisture becomes limiting in the third stage of crop growth. The third stage contributes most to *ETd* during the crop season, followed by the fourth stage contributing most of the remainder (Figure 4d). For soybean, the third stage contributes between 74% (Romania) to 84% (Italy) of *ETd*. For maize, the average contribution of the third stage to *ETd* is a bit lower, ranging between 64% in France and Romania to 68% in Italy and Hungary.

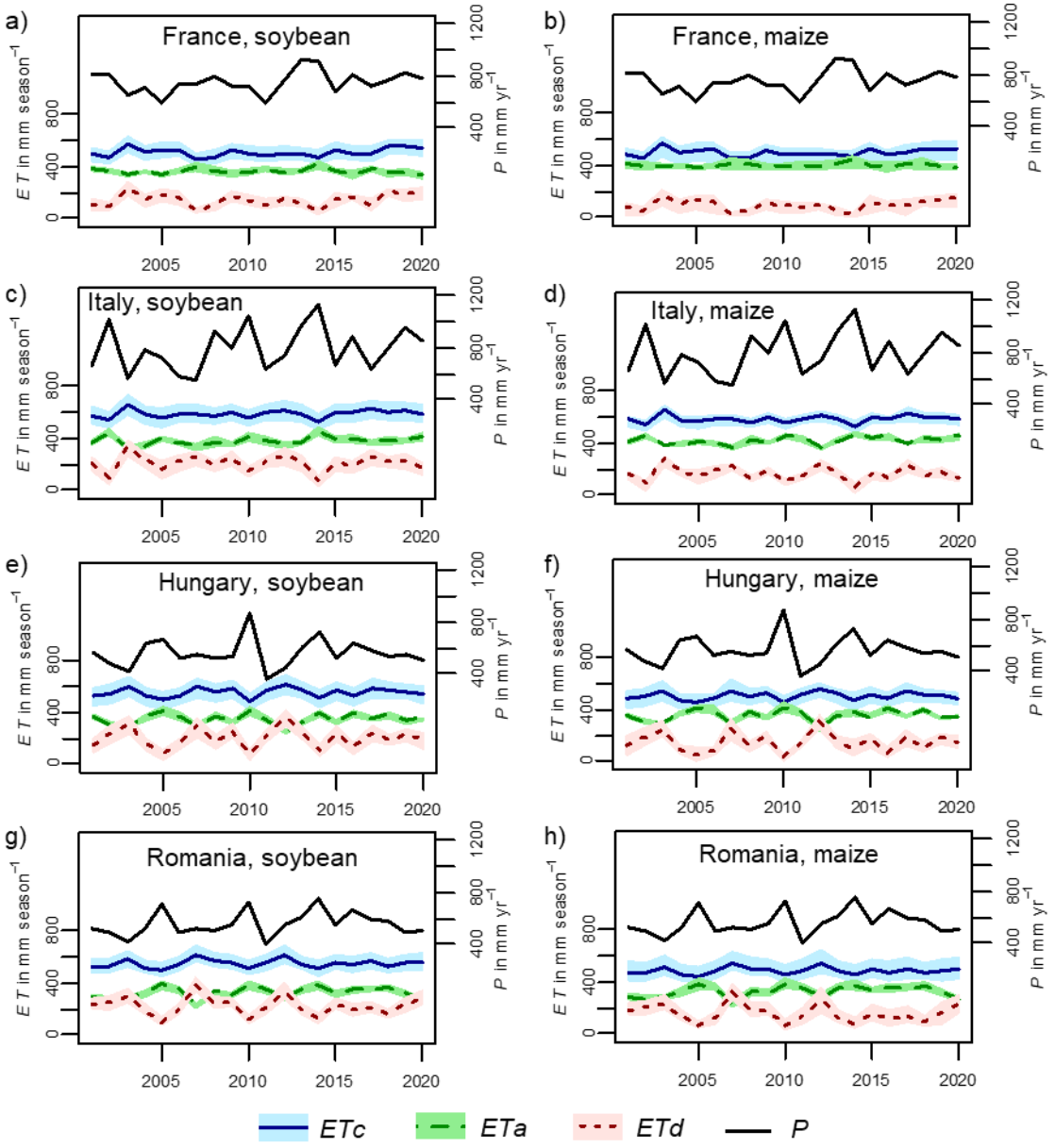

Figure 3. Simulated potential and actual evapotranspiration (*ETc* and *ETa*, respectively), and crop water deficit (*ETd*) for soybean and maize during the growing season vs. annual precipitation (*P*) in France, Italy, Hungary, and Romania. For *ETc*, *ETa*, and *ETd*, the colored areas and the lines give the range and mean of results over seven different crop calendar scenarios.

Table 4. Summary of simulation results for France, Italy, Hungary and Romania over the period 2001-2020: mean, standard deviation between years, standard deviation between crop calendars, and correlations between simulations.*

Parameter	Unit	France	Italy	Hungary	Romania
ETc_s	mm season^{-1}	513±31(39)	594±29(49)	555±36(49)	553±32(37)
ETa_s	mm season^{-1}	366±21(13)	382±33(13)	351±42(12)	329±44(12)
ETd_s	mm season^{-1}	146±48(27)	211±58(38)	204±75(38)	223±70(26)
ETc_m	mm season^{-1}	501±31(39)	590±28(24)	506±33(46)	489±28(47)
ETa_m	mm season^{-1}	404±13(16)	423±30(8)	357±43(11)	329±44(15)
ETd_m	mm season^{-1}	97±39(24)	167±53(17)	149±72(35)	160±66(33)
$\Delta ETc_{m\rightarrow s}$	mm season^{-1}	12±5(25)	4±6(36)	49±5(19)	64±4(32)
$\Delta ETa_{m\rightarrow s}$	mm season^{-1}	-38±13(11)	-40±15(9)	-7±15(7)	0±9(14)
$\Delta ETd_{m\rightarrow s}$	mm season^{-1}	50±16(17)	44±20(29)	55±17(14)	64±12(19)
P	mm yr^{-1}	754±88	797±172	563±112	558±95
ETc_s~ETa_s	-	-0.67	-0.71	-0.86	-0.74
ETc_m~ETa_m	-	-0.52	-0.65	-0.78	-0.66
ETc_s~P	-	n.s.	-0.62	-0.71	-0.53
ETa_s~P	-	n.s.	0.71	0.68	0.65
ETd_s~P	-	n.s.	-0.72	-0.72	-0.64
ETc_m~P	-	n.s.	-0.66	-0.67	-0.50
ETa_m~P	-	0.58	0.71	0.57	0.57
ETd_m~P	-	-0.48	-0.75	-0.65	-0.59

*Potential ET (*ETc*), actual ET (*ETa*) and crop water deficit (*ETd*) during cropping season of soybean ($_s$) and maize ($_m$) and the changes in these parameters when maize is converted to soybean ($\Delta ETc_{m\rightarrow s}$, $\Delta ETa_{m\rightarrow s}$, $\Delta ETd_{m\rightarrow s}$) are reported. The annual amounts of precipitation *P* are given for comparison. Values represent multi-annual means ± σ_{IAV} between years, while the numbers in brackets give standard deviation between crop calendar scenarios σ_{CC}. Finally, correlations between *ETc* and *ETa*, as well as between *P* and *ETc*, *ETa*, or *ETd*are reported as Pearson correlation coefficients.

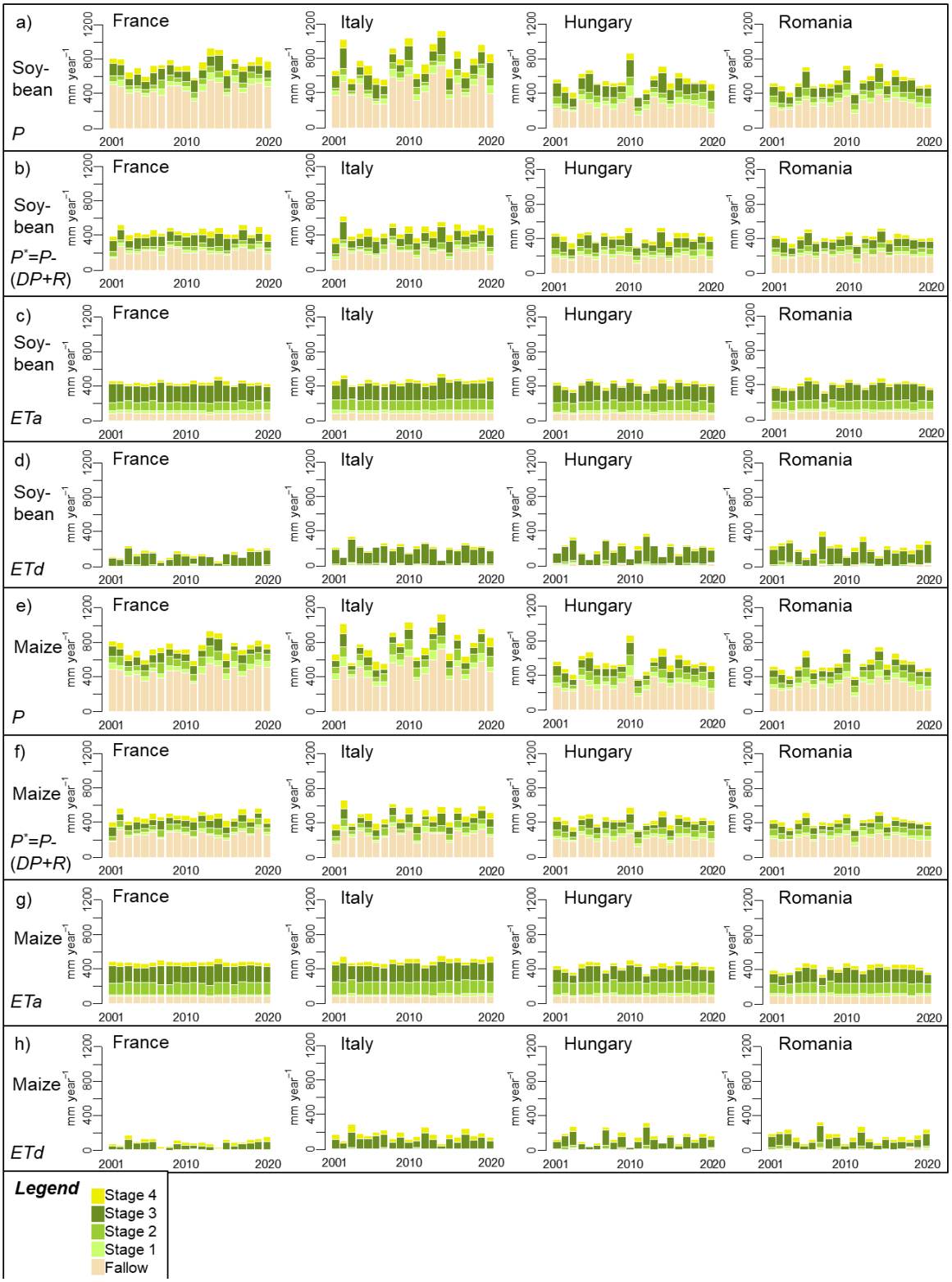

Figure 4: Values of precipitation *P*, amount of *P* not lost to runoff *R* and deep percolation *DP* (P^*), actual evapotranspiration *ETa*, and crop water deficit *ETd* for soybean and maize expressed by year and by season (four growth stages and fallow). For statistics with explicit values, see Table S1.

3.2 Impact of Crop Calendars

The seven crop calendar scenarios used in this study differ substantially with regard to sowing dates and season length (Table 5, Figure S2-S4). The choice of the crop calendar scenario has an impact on the simulations of *ETd*, *ETa* and *ETc* for both maize and soybean (Figures S5 and S6), and thus on the simulated changes of these three parameters when maize is converted to soybean ($\Delta ETd_{m\rightarrow s}$, $\Delta ETa_{m\rightarrow s}$, and $\Delta ETc_{m\rightarrow s}$, respectively, Figures S7). The standard deviations between results per crop calendar scenario σ_{CC} are quite important, as can be seen from Table 4. The relative size of σ_{CC} range between nearly one third (Romania) and about two thirds (Italy) of the average $\Delta ETd_{m\rightarrow s}$ per country. To explore the impact of the crop calendar scenarios on the simulations, we fitted regression models relating average values of average $\Delta ETd_{m\rightarrow s}$, $\Delta ETa_{m\rightarrow s}$, and $\Delta ETc_{m\rightarrow s}$ over the 20 year simulation period (per grid cell) to the differences in sowing date (Δt_{plant}) and season length (Δt_{seas}) induced by the crop substitution (Table 6). Our regression analysis was able to explain more than half of the variability of $\Delta ETd_{m\rightarrow s}$, $\Delta ETa_{m\rightarrow s}$, and $\Delta ETc_{m\rightarrow s}$. The estimated parameters in the regression for $\Delta ETd_{m\rightarrow s}$ appear to be a nearly linear combination of the parameters in regressions of $\Delta ETc_{m\rightarrow s}$ and $\Delta ETa_{m\rightarrow s}$ due to the fact that $\Delta ETd_{m\rightarrow s}$ is the difference between $\Delta ETc_{m\rightarrow S}$ and $\Delta ETa_{m\rightarrow s}$, just as *ETd* is the difference between *ETc* and *ETa*. The intercepts of the three equations indicate the main crop substitution effect, independently from the differences in crop calendars. These intercepts show that soybean has a higher *ETc* but a lower *ETa* than maize during the growing season, both leading to a higher *ETd* for soybean than for maize. The positive regression parameter assigned to Δt_{seas} indicates a tendency for $\Delta ETd_{m\rightarrow s}$ to be higher if the maize-soybean conversion leads to a longer growing period. This is due to the fact that *ETc* and *ETa* tend to increase with the length of the growing season. According to the crop calendars used in this study (Table 5), there appears to be a tendency for soybean to have a growing season as long as or longer than maize. The effect of Δt_{seas} on $\Delta ETc_{m\rightarrow s}$ is however substantially stronger than on $\Delta ETa_{m\rightarrow s}$, as can be seen from the parameters in Table 6, and which indicates an increasing water limitation of *ETa*. Accordingly, Δt_{seas} has also a positive effect of $\Delta ETd_{m\rightarrow s}$.

536 **Table 5.** Average Sowing Dates and Length of Growing Season of Soybean and Maize in the
537 four Countries where Maize-to-Soybean Conversions would be most Efficient.
538

	Sowing date (DOY)							
	Soybean				Maize			
Crop calendar	Fra	Ita	Hun	Rom	Fra	Ita	Hun	Rom
MIRCA, first day	121	121	121	121	91	91	121	121
MIRCA, central date	135	135	135	135	105	105	135	135
MIRCA, last day	150	150	150	150	120	120	151	151
JRC, first day	116	116	116	105	88	86	87	86
JRC, central date	133	133	133	120	119	110	118	117
JRC, last day	151	151	151	137	150	135	150	149
GGCMI	122	122	121	113	101	96	117	116
	Length of growing season (days)							
	Soybean				Maize			
Crop calendar	Fra	Ita	Hun	Rom	Fra	Ita	Hun	Rom
MIRCA, first day	154	154	154	154	154	154	154	154
MIRCA, central date	154	154	154	154	154	154	154	154
MIRCA, last day	154	154	154	154	154	154	154	154
JRC, first day	170	170	170	148	169	161	153	122
JRC, central date	170	170	170	148	169	161	153	122
JRC, last day	170	170	170	148	169	161	153	122
GGCMI	160	160	162	124	156	149	138	120

539
540 **Table 6.** Maize-to-Soybean Conversion Impact on *ETd*, *ETc*, and *ETa* as Explained by Changes
541 in Sowing Date (Δt_{plant}) and Season Length (Δt_{seas}).*
542

Dependent variable	Intercept	Δt_{plant}		Δt_{seas}		RMSE
		Slope	*r*	Slope	*r*	
$\Delta ETd_{m\rightarrow s}$	61.2±0.4	-1.06±0.00	-0.57	1.25±0.01	0.52	30.6
$\Delta ETc_{m\rightarrow s}$	42.5±0.2	-1.65±0.00	-0.75	2.13±0.01	0.72	35.7
$\Delta ETa_{m\rightarrow s}$	18.2±0.3	-0.61±0.00	-0.70	0.90±0.00	0.68	12.5

543 *Results from multiple linear regression with random effect. Dependent variables, intercept and RMSE
544 are in mm season^{-1}. Units of Δt_{plant} and Δt_{seas} are day of the year and days respectively. For both variables,
545 the partial correlation *r* is given.
546
547 Similarly, negative regression parameters assigned to Δt_{plant} indicate that $\Delta ETc_{m\rightarrow s}$ and $\Delta ETa_{m\rightarrow s}$
548 decrease if soybean is sown later than maize and increase if soybean is sown earlier. This can be
549 explained by the fact that the later soybean or maize are sown, the longer the growing season will
550 extend into autumn, when *ETc* tends to be much lower than during the hot summer months.

Again, this effect is stronger for $\Delta ETc_{m\rightarrow s}$ than for $\Delta ETa_{m\rightarrow s}$, and thus Δt_{plant} has a negative effect on $\Delta ETd_{m\rightarrow s}$ as well. As we see from Table 5, there is a strong tendency for soybean to be sown later than maize, which has an attenuating effect on $\Delta ETd_{m\rightarrow s.}$ Interestingly, the partial correlations for Δt_{plant} are about as strong as for Δt_{seas}, which means that both season length and sowing date have a similar importance in changing crop water needs, consumption and deficits.

3.3 Sensitivity Analysis to Model Parameters

Figure 5 shows the sensitivity of simulated $\Delta ETa_{m\rightarrow s}$, $\Delta ETc_{m\rightarrow s}$, and $\Delta ETd_{m\rightarrow s}$ to different model parameters. Sensitivities were computed by replacing the parameter values of soybean by the values derived for maize. All sensitivity values (mean and σ_{IAV}) are shown in Table S2 in the supplemental material. Note that the crop calendar used for this sensitivity analysis, GGCMI, gives very similar sowing and harvest dates from soybean and maize, and for that reason the crop calendar appears to have a minor effect on the result (Table 5, Figures S2-S4). Only in Hungary, where the GGCMI crop calendar gives a growing season for soybean which is about 3 weeks longer than that for maize, we see an impact on $\Delta ETa_{m\rightarrow s}$ (+21±11 mm season^{-1}), $\Delta ETc_{m\rightarrow s}$ (+47±10 mm season^{-1}), and $\Delta ETd_{m\rightarrow s}$ (+26±18 mm season^{-1}) (mean and σ_{IAV}, Table S2).
The different crop coefficients (*Kc*) appear to be the major reason for an increase in *ETc* under soybean, with values of $\Delta ETc_{m\rightarrow s,Kc}$ ranging from +35±2 mm season^{-1} in Romania to +48±3 mm season^{-1} in Italy (Table S2). In contrast, the shorter root depth for soybean vs. maize (1.3 m vs. 1.7 m, respectively) appears to be the main driver of the simulated reduction in *ETa* when maize is converted to soybean. Interestingly, this effect seems to be much stronger in France and Italy ($\Delta ETa_{m\rightarrow s,Droot}$ of -39±7 and -41±8 mm season^{-1}, respectively), and relatively weak in Hungary and Romania ($\Delta ETa_{m\rightarrow s,Droot}$ of -17±15 and -12±8 mm season^{-1}, respectively, Table S2). For *ETd*, it seems to be the combination of crop coefficients and root depth that lead to an increase when maize is converted to soybean, through the effect of these parameters on *ETc* and *ETa*, respectively. The impact of the different crop coefficients on crop water deficit, $\Delta ETd_{m\rightarrow s,Kc}$, ranges from +30±5 mm season^{-1} in Romania and +30±9 mm season^{-1} in France to +41±8 mm season^{-1} in Hungary. The impact of the difference in root depth on crop water deficit, $\Delta ETd_{m\rightarrow s,Droot}$, ranges from +12±8 mm season^{-1} in Romania to +38±8 mm season^{-1} in Italy (Table S2). Moreover, while differences in root depth are responsible for half of the total $\Delta ETd_{m\rightarrow s}$ in France and Italy, this parameter contributes for less than one fourth of the total $\Delta ETd_{m\rightarrow s}$ in Hungary and Romania.

585

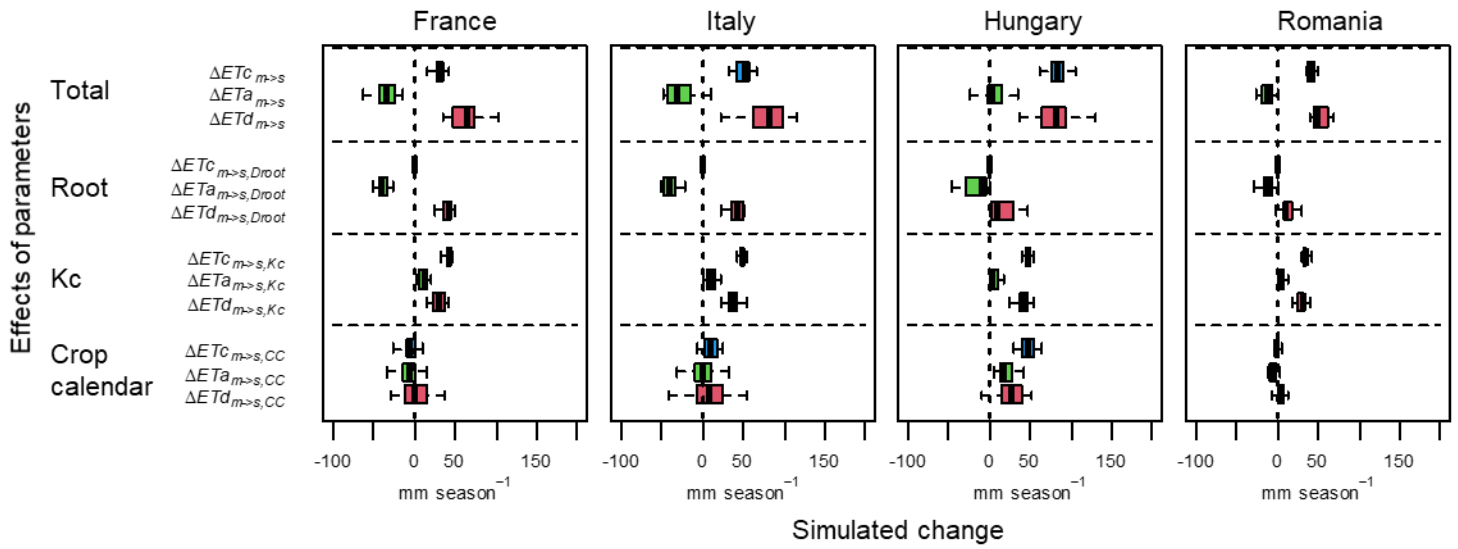

586
587

588 **Figure 5**. Simulated Change in Potential ET ($\Delta ETc_{m\rightarrow s}$, blue boxes), Actual ET ($\Delta ETa_{m\rightarrow s}$, green boxes) and Crop Water Deficit
589 ($\Delta ETd_{m\rightarrow s}$, red boxes) when Maize would be Converted to Soybean, Quantitatively Detailing the Contributions of assumed Root
590 Depth ($_{Droot}$), Crop Coefficents ($_{Kc}$), and Crop Calendars ($_{CC}$).*
591 *Box plots represent the variability of annual values over the 20 year simulation period, with median, interquartile range and total
592 range of values. For this sensitivity test, the GGCMI crop calendar was used.

4 Discussion

4.1 Interpretation of results

For our simulations, we assumed that all maize would be converted to soybean where the potential soybean yield would be 1.5 t $ha^{-1}yr^{-1}$ and higher. The four countries of France, Italy, Hungary and Romania would contribute 80% of that soybean production. We are well aware that a complete conversion of maize to soybean is not a realistic scenario. But assuming a conversion proportional to the total maize area in regions with a reasonably high expected soybean yield, the relative importance of these four countries seems valid for an analysis of the impact of a maize-to-soybean conversion on the climatic crop water demand/deficit within the EU. A sensitivity analysis using alternative thresholds of soybean yield of 1.0 and 2.0 t $ha^{-1}yr^{-1}$ shows that results presented in this paper are not affected by this threshold value (Table S3).

We found that the major part of crop water deficit occurs in the third of the four crop growth stages considered in our model (Figure S8), i.e. the mid-season from flowering to ripening of fruits and seeds, which would thus be the right time to irrigate. In France, Italy, and Hungary, the average timing of this third stage soybean development is between early July and mid-September. In Romania, the average timing of that stage is late June to the end of August. For maize, the duration of this third stage is about three weeks shorter, and ends already in the second half of August in all four countries. During these summer months, abstractions of water from surface- and groundwater bodies are increased, in particular for crop irrigation, while renewal of freshwater resources is reduced (Kristensen et al., 2018). This is even more the case in countries such as France and Italy where irrigation plays an important role (Kristensen et al., 2018).

For Italy, Hungary, and Romania we predict average crop water deficit for soybean of slightly above 200 mm $season^{-1}$, which compares well with water amounts applied for (close to) full irrigation of soybeans reported for fields in Croatia (Markovic et al. 2016) and Serbia (Pejic et al. 2012), which lie geographically between these three countries. We saw that *ETd* would be higher under soybean than under maize in all four countries, but due to different reasons. We saw that the choice of crop calendars has a significant impact on simulation results. Nevertheless, under all scenarios, we simulate an increase in crop water deficit for a maize-to-soybean conversion. In Italy and France, $\Delta ETd_{m \rightarrow s}$ was mainly driven by $\Delta ETa_{m \rightarrow s}$. According to our simulations, a maize-to-soybean conversion would lower *ETa* by on average by ~10% in these two countries, which is comparable to what was found by Suyker & Verma (2009) in Nebraska under rainfed conditions. In Hungary and Romania, in contrast, $\Delta ETd_{m \rightarrow s}$ was mainly driven by $\Delta ETc_{m \rightarrow s}$, with a maize-to-soybean conversion increasing *ETc* by ~10%. Interestingly, the predicted $\Delta ETa_{m \rightarrow s}$ was minor to negligible in these two countries. That indicates that available soil water is more limiting in these two countries, not permitting for higher *ETa* under maize as predicted for France and Italy.

Our sensitivity analysis showed that positive $\Delta ETc_{m \rightarrow s}$ was largely caused by differences in crop coefficients, while the negative $\Delta ETa_{m \rightarrow s}$ was caused by differences in assumed root zone depth.

The crop coefficients used by the FAO56 approach are based on numerous empirical findings. While some variability is to be expected among sites and varieties of maize and soybean, we can assume that the FAO56 parametrization is representative for European sites. Even for soybean, which is still not a very common crop in Europe, empirical studies from Hungary (Anda et al., 2020) and Croatia (Marković et al., 2016) confirm the applicability of FAO56 crop coefficients in Europe. The study by Anda et al. (2020) even showed that crop coefficients are very similar

between more and less drought tolerant varieties of soybean (*Sinara* and *Sigalia*, respectively, Figure S9).

In contrast, generally assuming a rooting zone depth of 1.70 m for maize may appear unrealistic, in particular in areas where root penetrable soil depth is limited. These values may represent rather the maximum root zone depth under favorable soil conditions. Ordóñez et al. (2018) suggest that in many areas, soybean and maize would rather develop a similar root depth. One should thus be cautious regarding the effect of prescribed different root zone depth on our simulation results. Using the default parameters of FAO56 approach, we simulate area weighted, average ($\pm\sigma_{IAV}$) $\Delta ETd_{m\rightarrow s}$ of 49.0±22.1 mm season^{-1} across the EU, which represents an increase in crop water deficit of 39% relative to maize. Using the same root zone depth of 1.30 m for soybean and maize, simulated $\Delta ETd_{m\rightarrow s}$ is reduced to 28.2±18.3 mm season^{-1}. This would however still represent an increase in crop water deficit by 19% relative to maize.

As shown for the examples of Hungary and Romania, differences in root zone depth does not seem to affect $\Delta ETd_{m\rightarrow s}$ in dryer climates were soil moisture availability is more limiting and does not permit for higher *ETa* under maize even if the roots reach substantially deeper soil layers. This also means that concerning the uncertainty arising from the assumed root depth, our simulation results are more robust for Hungary and Romania than they are for France and Italy.

4.2 Model Limitations and Perspectives

The methodological approach of our study is simple and afflicted by a number of shortcomings, which we would like to point out shortly. First of all, while we quantify the crop water deficit, our approach is not able to quantify the effects of crop water deficit and realized, actual ET on yields. Quantification of yield gaps caused by water shortage and of increases in yields through irrigation would help to better assess the actual need for irrigation (Grassini et al. 2011b, 2014). Similarly, while later sowing dates and shorter growing periods were found to reduce crop water deficits, they may also decrease yields (Serafin-Andrzejewska et al. 2021; Mourtzinis et al., 2019). Consideration of all costs involved in irrigation and changing revenues from increased crop yield would be necessary to assess whether and in how far irrigation would be economically worthwhile. Moreover, while our approach to calculate crop water deficit implies a baseline of full irrigation, reasonable yield increases for soybean could still be achieved through deficit irrigation (Karam et al., 2005), i.e. with less than full irrigation. Finally, costs of water and market prices of crops may change over time (Kim & Kaluarachchi, 2016), which would make such an assessment further challenging.

More importantly, our approach is limited in the sense that different management practices that could affect water needs, consumption and deficits are not represented in our model. We used standard parametrization of crop coefficients following FAO56 in combination with seven different prescribed crop calendar scenarios. However, it is not clear how the choice of different cultivars may affect actual sowing dates, length of growing season, and the actual crop coefficients and root depths. This is especially the case under European conditions where soybean is a relatively new crop and breeders are actively working to develop new varieties adapted to local conditions, taking advantage of the wide range of variations in existing so-called soybean maturity groups and associated lengths of the growing cycle (Kurasch et al. 2017). Indeed, a locally adapted choice of cultivars with specific sowing dates would likely reduce crop water deficits and related yield gaps, as shown by recent work on soybean in the US Corn Belt (Andrade et al. 2022) and China (He et al. 2017). Further, we do not account for effects of differences in sowing density that would affect *ETc*, *ETa* and *ETd* (Di Mauro et al. 2019,

Holshouser and Whittaker 2002). Also the effect of different tillage strategies and/or mulching on soil evaporation losses is not taken into account. These management strategies would however be an interesting lever to reduce crop water deficits (Jin et al., 2007).

Further, as discussed in the preceding subsection, our model is limited by assuming everywhere the same maximum root depth, although rooting depth may be limited by root penetrable soil depth or ground water table that may vary drastically between different locations (Chen et al. 2021). To our knowledge, no reliable dataset of root penetrable soil depth exists at European scale, as soil depth is still very poorly predicted by digital soil mapping techniques (Chen et al. 2022). Future advances in mapping rootable soil depth in Europe would thus benefit strongly to any work aiming at assessing future crop water needs in relation to the availability of renewable water resources under climate change. Moreover, maximum root depth is not only limited by rootable soil depth but also varies with climatic conditions (Benjamin and Nielsen 2006), cultivars (Fried et al. 2018, Liu et al. 2021) and management practices (Fan et al., 2017; Ordóñez et al., 2018). Important improvements to our current crop root modeling approach would be needed to simulate such differences in root growth. This deserves further research. Our results revealed a large impact of the maximum root depth parameter on actual ET and water deficit of soybean. This reinforces the relevance of on-going work aiming at breeding soybean varieties adapted to drought with a focus on roots traits (Bishop and Lynch 2015, Xiong te al. 2021).

Finally, our model follows a prescribed phenological development of the crop plants, not taking into account delays in plant development, due to e.g. water shortage, and not allowing for flexibility in sowing and harvest dates. Differences between existing crop calendars likely represents a mix of a certain flexibility in sowing and harvest dates on one hand, and a limited reliability of these datasets on the other hand. A better representation of the effects of management practices on actual crop water needs and deficits could help to better assess the implications of a maize-to-soybean conversion on irrigation demands.

5 Conclusion and Outlook

We predict an increase in crop water deficit following a maize-to-soybean conversion in France, Italy, Hungary, and Romania. The country-average increases in crop water deficit are rather similar, ranging between 44±20 mm season^{-1} in Italy and 64±12mm season^{-1} in Romania and representing an increase of about 21-34% of water deficit compared to rainfed maize. If the entire area suitable for maize to crop substitution within the EU is taken as reference, the increase in crop water deficit is even 39% relative to that of rainfed maize. The country-average crop water deficit of new soybean fields would be substantially lower in France (~150 mm season^{-1}) than for the other three countries (200-220 mm season^{-1}).

Our results have however to be seen critically in the light of the uncertainties existing on key parameter values having strong impacts on water deficit estimations, in particular on maximum root depth. Our estimates of an increase in crop water deficit through a maize-to-soybean conversion only holds true if we assume a substantially higher max root depth for maize than for soybean (as 1.7 m vs. 1.3 m following the default values of the FAO56 approach followed in this study). There is however doubt that maize will often develop a higher root depth than soybean, in particular if rootable soil depth is limited. Thus, more research on attained root depth of maize vs. soybean across Europe is needed to better constraint the potential impact of maize-to-soybean conversion on the crop water deficit. Finally, our simulation results suggest that crop water deficits can be decreased by choosing later sowing dates, but probably at the costs of lower water-limited yields. While this appears a promising strategy to decrease crop water deficit, an

assessment of how the choice of sowing dates would affect yields would help to better evaluate the agronomic practicability.

733 **Appendix**

734

735 Table A1: Variables used in the study.

Code	Variable name
D_{root}	Depth of rootzone, time-variant
D_{soil}	Depth of soil column, fixed
D_{top}	Depth of topsoil, fixed
DI	Deep infiltration from top- to subsoil
DP	Deep percolation out of subsoil
Ea	Actual evaporation
Ea_{top}	Actual evaporation from topsoil
Ec	Potential evaporation
ET	Evapotranspiration
ET0	Reference *ET* (i.e. potential *ET* of a reference crop)
ETa	Actual evapotranspiration
ETc	Potential evapotranspiration
ETd	Crop water deficit (=*ETc*-*ETa*)
FC	Field capacity
FC_{top}	Field capacity of topsoil
Kc	Crop coefficient relating *ETc* to *ET0*
Kcb	Partial crop coefficient relating *Tc* to *ET0*
Ke	Partial crop coefficient relating *Ec* to *ET0*
Kr	Coefficient expressing limitation for Ea_{top} by water availability
Ks	Coefficient expressing limitation for Ta by water availability
P	Precipitation
p	Parameter used in the calculation of *Ks*
pstd	Crop specific constant used in the calculation of *p*
R	Surface runoff
REW	Water in topsoil readily available for evaporation
S_{root}	Water storage in root zone
S_{sub}	Water storage in subsoil
S_{top}	Water storage in topsoil
Ta	Actual transpiration
Ta_{sub}	Actual transpiration from subsoil
Ta_{top}	Actual transpiration from topsoil
Tc	Potential transpiration, crop specific
PWP	Permanent wilting point
PWP_{top}	Permanent wilting point in topsoil

736

Acknowledgements

This work was supported by the CLAND convergence institute (16-CONV-0003) funded by the French National Research Agency (ANR).

References

Agam (Ninari), N., Berliner, P. R., Zangvil, A., and Ben-Dor, E. (2004), Soil water evaporation during the dry season in an arid zone, *J. Geophys. Res.*, 109, D16103, doi:10.1029/2004JD004802.

Allen, R. G., Pereira, L. S., Raes, D., & Smith, M. (1998). *Crop Evapotranspiration (guidelines for computing crop water requirements). FAO Irrigation and Drainage Paper 56.*

Anda, A., Simon, B., Soos, G., Teixeira da Silva, J. A., Farkas, Z., & Menyhart, L. (2020). Assessment of soybean evapotranspiration and controlled water stress using traditional and converted evapotranspirometers. *Atmosphere*, *11*(8). https://doi.org/10.3390/ATMOS11080830

Andrade, J. F., Mourtzinis, S., Edreira, J. I. R., Conley, S. P., Gaska, J., Kandel, H. J., ... & Grassini, P. (2022). Field validation of a farmer supplied data approach to close soybean yield gaps in the US North Central region. Agricultural Systems, 200, 103434.

Arino, O., Ramos Perez, J. J., Kalogirou, V., Bontemps, S., Defourny, P., & Van Bogaert, E. (2012, August 23). Global Land Cover Map for 2009 (GlobCover 2009). PANGAEA. https://doi.org/10.1594/PANGAEA.787668

Behnke, G. D., Zuber, S. M., Pittelkow, C. M., Nafziger, E. D., & Villamil, M. B. (2018). Long-term crop rotation and tillage effects on soil greenhouse gas emissions and crop production in Illinois, USA. *Agriculture, Ecosystems & Environment*, *261*, 62–70. https://doi.org/10.1016/j.agee.2018.03.007

Benjamin, J. G., & Nielsen, D. C. (2006). Water deficit effects on root distribution of soybean, field pea and chickpea. Field crops research, 97(2-3), 248-253.

Bishopp, A., Lynch, J. The hidden half of crop yields. Nature Plants 1, 15117 (2015). https://doi.org/10.1038/nplants.2015.117

Cernay, C., Makowski, D. & Pelzer, E. (2018). Preceding cultivation of grain legumes increases cereal yields under low nitrogen input conditions. *Environ Chem Lett* **16**, 631–636. https://doi.org/10.1007/s10311-017-0698-z

Chen, S., Richer-de-Forges, A. C., Mulder, V. L., Martelet, G., Loiseau, T., Lehmann, S., & Arrouays, D. (2021). Digital mapping of the soil thickness of loess deposits over a calcareous bedrock in central France. Catena, 198, 105062.

Chen, S., Arrouays, D., Mulder, V. L., Poggio, L., Minasny, B., Roudier, P., ... & Walter, C. (2022). Digital mapping of GlobalSoilMap soil properties at a broad scale: A review. Geoderma, 409, 115567.

Debaeke, P., Forslund, A., Guyomard, H., Schmitt, B., Tibi, A. (2022). Could domestic soybean production avoid Europe's protein imports in 2050? OCL 29, Article no. 38, https://doi.org/10.1051/ocl/2022031

Di Mauro, G., Borrás, L., Rugeroni, P., & Rotundo, J. L. (2019). Exploring soybean management options for environments with contrasting water availability. Journal of Agronomy and Crop Science, 205(3), 274-282.

European Commission. (2020). Farm to Fork Strategy. For a fair, healthy and environmentally-friendly food system. Retrieved June 21, 2022, from https://ec.europa.eu/food/system/files/2020-05/f2f_action-plan_2020_strategy-info_en.pdf

European Commission. (2022). EUROSTAT. Retrieved May 13, 2022, from https://ec.europa.eu/eurostat/data/database

Fan, Y., Miguez-Macho, G., Jobbágy, E. G., Jackson, R. B., & Otero-Casal, C. (2017). Hydrologic regulation of plant rooting depth. *Proceedings of the National Academy of Sciences*, *114*(40), 10572–10577. https://doi.org/10.1073/pnas.1712381114

Fearnside, P. M. (2001). Soybean cultivation as a threat to the environment in Brazil. *Environmental Conservation*, *28*(1), 23–38. https://doi.org/10.1017/S0376892901000030

Fried, H. G., Narayanan, S., & Fallen, B. (2018). Characterization of a soybean (Glycine max L. Merr.) germplasm collection for root traits. PLoS One, 13(7), e0200463.

Grassini, P., Torrion, J. A., Yang, H. S., Rees, J., Andersen, D., Cassman, K. G., & Specht, J. E. (2015). Soybean yield gaps and water productivity in the western U.S. Corn Belt. *Field Crops Research*, *179*, 150–163. https://doi.org/10.1016/j.fcr.2015.04.015

Grassini, P., Yang, H., Irmak, S., Thorburn, J., Burr, C., & Cassman, K. G. (2011). High-yield irrigated maize in the Western US Corn Belt: II. Irrigation management and crop water productivity. Field crops research, 120(1), 133-141.

Grassini, P., Torrion, J. A., Cassman, K. G., Yang, H. S., & Specht, J. E. (2014). Drivers of spatial and temporal variation in soybean yield and irrigation requirements in the western US Corn Belt. Field Crops Research, 163, 32-46.

Guilpart, N., Iizumi, T., & Makowski, D. (2022). Data-driven projections suggest large opportunities to improve Europe's soybean self-sufficiency under climate change. *Nature Food*, *3*(4), 255–265. https://doi.org/10.1038/s43016-022-00481-3

Grassini, P., Specht, J. E., Tollenaar, M., Ciampitti, I., & Cassman, K. G. (2015). High-yield maize–soybean cropping systems in the US Corn Belt. In Crop physiology (pp. 17-41). Academic Press.

Harlander, S. K. (2002). Safety Assessments and Public Concern for Genetically Modified Food Products: The American View. *Toxicologic Pathology*, *30*(1), 132–134. https://doi.org/10.1080/01926230252824833

He, J., Du, Y. L., Wang, T., Turner, N. C., Yang, R. P., Jin, Y., ... & Li, F. M. (2017). Conserved water use improves the yield performance of soybean (Glycine max (L.) Merr.) under drought. Agricultural Water Management, 179, 236-245.

Holshouser, D. L., & Whittaker, J. P. (2002). Plant population and row- spacing effects on early soybean production systems in the Mid- Atlantic USA. Agronomy Journal, 94(3), 603-611.

Jägermeyr, J., Müller, C., Ruane, A. C., Elliott, J., Balkovic, J., Castillo, O., et al. (2021). Climate impacts on global agriculture emerge earlier in new generation of climate and crop models. *Nature Food*, *2*(11), 873–885. https://doi.org/10.1038/s43016-021-00400-y

Jin, H., Hongwen, L., Xiaoyan, W., McHugh, A. D., Wenying, L., Huanwen, G., & Kuhn, N. J. (2007). The adoption of annual subsoiling as conservation tillage in dryland maize and wheat cultivation in northern China. *Soil and Tillage Research*, *94*(2), 493–502. https://doi.org/10.1016/j.still.2006.10.005

Karlsson, J. O., Parodi, A., Van Zanten, H. H., Hansson, P. A., & Röös, E. (2021). Halting European Union soybean feed imports favours ruminants over pigs and poultry. *Nature Food*, 2(1), 38-46. https://doi.org/10.1038/s43016-020-00203-7

Karam, F., Masaad, R., Sfeir, T., Mounzer, O., & Rouphael, Y. (2005). Evapotranspiration and seed yield of field grown soybean under deficit irrigation conditions. *Agricultural Water Management*, *75*(3), 226–244. https://doi.org/10.1016/j.agwat.2004.12.015

Karges, K., Bellingrath-Kimura, S. D., Watson, C. A., Stoddard, F. L., Halwani, M., & Reckling, M. (2022). Agro-economic prospects for expanding soybean production beyond its current northerly limit in Europe. *European Journal of Agronomy*, *133*, 126415. https://doi.org/10.1016/j.eja.2021.126415

Kim, D., & Kaluarachchi, J. J. (2016). A risk-based hydro-economic analysis for land and water management in water deficit and salinity affected farming regions. *Agricultural Water Management*, *166*, 111–122. https://doi.org/10.1016/j.agwat.2015.12.019

Kristensen, P., Whalley, C., Zal, F. N. N., & Christiansen, T. (2018). European waters assessment of status and pressures 2018. *EEA Report*, (No.7/2018), 85 pp.

Kurasch, A. K., Hahn, V., Leiser, W. L., Vollmann, J., Schori, A., Bétrix, C., & Mayr, B. (2017). Identification of mega-environments in Europe and effect of allelic variation at maturity E loci on adaptation of European soybean. Plant Cell and Environment, 0000, 1–14. https://doi.org/10.1111/pce.12896

Langthaler, E. (2020). Broadening and deepening: Soy expansions in a world-historical perspective. *Historia Ambiental Latinoamericana y Caribena*, *10*(1), 244–277. https://doi.org/10.32991/2237-2717.2020V10I1.P244-277

Liu, S., Begum, N., An, T., Zhao, T., Xu, B., Zhang, S., ... & Chen, Y. (2021). Characterization of root system architecture traits in diverse soybean genotypes using a semi-hydroponic system. *Plants*, 10(12), 2781.

MacBean, N., Scott, R. L., Biederman, J. A., Ottlé, C., Vuichard, N., Ducharne, A., Kolb, T., Dore, S., Litvak, M., and Moore, D. J. P. (2020): Testing water fluxes and storage from two hydrology configurations within the ORCHIDEE land surface model across US semi-arid sites, *Hydrol. Earth Syst. Sci.*, 24, 5203–5230, https://doi.org/10.5194/hess-24-5203-2020.

Marković, M., Josipović, M., Ravlić, M., Josipović, A., & Zebec, V. (2016). Deficit irrigation of soybean (Glycinemax. (L.) Merr.) based on monitoring of soil moisture, in sub-humid area of eastern croatia. *Romanian Agricultural Research*, *2016*(33). Retrieved from

https://www.scopus.com/inward/record.uri?eid=2-s2.0-84960387417&partnerID=40&md5=d6ddfa985608e6317d963719da08fdc1

Martin, N. (2015). Domestic soybean to compensate the European protein deficit: illusion or real market opportunity? *OCL*, *22*(5), D502. https://doi.org/10.1051/ocl/2015032

Mourtzinis, S., Specht, J. E., & Conley, S. P. (2019). Defining optimal soybean sowing dates across the US. Scientific Reports, 9(1), 2800. https://doi.org/10.1038/s41598-019-38971

Nachtergaele, F., van Velthuizen, H., Verelst, L., Batjes, N. H., Dijkshoorn, K., van Engelen, V. W. P., et al. (2010). The Harmonized World Soil Database. In *Proceedings of the 19th World Congress of Soil Science, Soil Solutions for a Changing World, Brisbane, Australia, 1-6 August 2010* (pp. 34–37). Brisbane, Australia: R.J. Gilkes & N. Prakongkep.

Nemecek, T., von Richthofen, J.-S., Dubois, G., Casta, P., Charles, R., & Pahl, H. (2008). Environmental impacts of introducing grain legumes into European crop rotations. European Journal of Agronomy, 28(3), 380–393. https://doi.org/10.1016/j.eja.2007.11.004

Nepstad, D., McGrath, D., Stickler, C., Alencar, A., Azevedo, A., Swette, B., et al. (2014). Slowing Amazon deforestation through public policy and interventions in beef and soy supply chains. *Science*, *344*(6188), 1118–1123. https://doi.org/10.1126/science.1248525

Ordóñez, R. A., Castellano, M. J., Hatfield, J. L., Helmers, M. J., Licht, M. A., Liebman, M., et al. (2018). Maize and soybean root front velocity and maximum depth in Iowa, USA. *Field Crops Research*, *215*, 122–131. https://doi.org/10.1016/j.fcr.2017.09.003

Pereira, L.S., Paredesa, P., Jovanovic, N. (2020). Soil water balance models for determining crop water and irrigation requirements and irrigation scheduling focusing on the FAO56 method and the dual Kc approach. *Agricultural Water Management* 241, Artcile no. 106357. https://doi.org/10.1016/j.agwat.2020.106357

Portmann, F. T., Siebert, S., & Döll, P. (2010). MIRCA2000—Global monthly irrigated and rainfed crop areas around the year 2000: A new high-resolution data set for agricultural and hydrological modeling. *Global Biogeochemical Cycles*, *24*(1). https://doi.org/10.1029/2008GB003435

Raes, D., Geerts, S., Kipkorir, E., Wellens, J., & Sahli, A. (2006). Simulation of yield decline as a result of water stress with a robust soil water balance model. *Agricultural Water Management*, *81*(3), 335–357. https://doi.org/10.1016/j.agwat.2005.04.006

Raes, D., Steduto, P., Hsiao, T. C., & Fereres, E. (2009). AquaCrop—The FAO Crop Model to Simulate Yield Response to Water: II. Main Algorithms and Software Description. *Agronomy Journal*, *101*(3), 438–447. https://doi.org/10.2134/agronj2008.0140s

Reckling, M., Albertsson, J., Vermue, A., Carlsson, G., Watson, C. A., Justes, E., ... & Topp, C. F. (2022). Diversification improves the performance of cereals in European cropping systems. *Agronomy for Sustainable Development*, *42*(6), 118. https://doi.org/10.1007/s13593-022-00850-z

Rosa, R. D., Ramos, T. B., & Pereira, L. S. (2016). The dual Kc approach to assess maize and sweet sorghum transpiration and soil evaporation under saline conditions: Application of the SIMDualKc model. *Agricultural Water Management*, *177*, 77–94. https://doi.org/10.1016/j.agwat.2016.06.028

Rüdelsheim, P. L. J. & Smets, G. (2012). Baseline information on agricultural practices in the EU soybean (Glycine max (L.) Merr.). Perseus BVBA.

Sacks, W. J., Deryng, D., Foley, J. A., & Ramankutty, N. (2010). Crop planting dates: an analysis of global patterns. *Global Ecology and Biogeography*, *19*(5), 607–620. https://doi.org/10.1111/j.1466-8238.2010.00551.x

Serafin-Andrzejewska, M., Helios, W., Jama-Rodzeńska, A., Kozak, M., Kotecki, A., & Kuchar, L. (2021). Effect of sowing date on soybean development in south-western Poland. Agriculture, 11(5), 413. https://doi.org/10.3390/agriculture11050413

Sheikh, V., Visser, S., & Stroosnijder, L. (2009). A simple model to predict soil moisture: Bridging Event and Continuous Hydrological (BEACH) modelling. *Environmental Modelling & Software*, *24*(4), 542–556. https://doi.org/10.1016/j.envsoft.2008.10.005

Siebert, S., & Döll, P. (2010). Quantifying blue and green virtual water contents in global crop production as well as potential production losses without irrigation. *Green-Blue Water Initiative (GBI)*, *384*(3), 198–217. https://doi.org/10.1016/j.jhydrol.2009.07.031

Tóth, B., Weynants, M., Pásztor, L., & Hengl, T. (2017). 3D soil hydraulic database of Europe at 250 m resolution. *Hydrological Processes*, *31*(14), 2662–2666. https://doi.org/10.1002/hyp.11203

USDA NRCS. (2004). *National Engineering Handbook, Part 630 Hydrology.*

Wilcox, J. R. (2016). World distribution and trade of soybean. In *Soybeans: Improvement, Production, and Uses* (pp. 1–14). https://doi.org/10.2134/agronmonogr16.3ed.c1

Xiong, R., Liu, S., Considine, M. J., Siddique, K. H., Lam, H. M., & Chen, Y. (2021). Root system architecture, physiological and transcriptional traits of soybean (Glycine max L.) in response to water deficit: A review. Physiologia Plantarum, 172(2), 405-418.

Zajac, Z., Gomez, O., Gelati, E., van der Velde, M., Bassu, S., Ceglar, A., et al. (2022). Estimation of spatial distribution of irrigated crop areas in Europe for large-scale modelling applications. *Agricultural Water Management*, *266*, 107527. https://doi.org/10.1016/j.agwat.2022.107527

Zander, P., Amjath-Babu, T. S., Preissel, S., Reckling, M., Bues, A., Schläfke, N., et al. (2016). Grain legume decline and potential recovery in European agriculture: a review. *Agronomy for Sustainable Development*, *36*(2), 26. https://doi.org/10.1007/s13593-016-0365-y